Cutinase, a Lipolytic Enzyme with a Preformed Oxyanion Hole[†,‡]

Chrislaine Martinez,[§] Anne Nicolas,[§] Herman van Tilbeurgh,[§] Marie-Pierre Egloff,[§] Claire Cudrey,[∥] Robert Verger,[∥] and Christian Cambillau*[,§]

Laboratoire de Cristallisation et Cristallographie des Macromolécules Biologiques; URA 1296-CNRS, Faculté de Médecine Nord, 13916 Marseille Cedex 20, France, and Laboratoire de Lipolyse Enzymatique, GDR 1000-CNRS, 31 Chemin Joseph Aiguier, 13402 Marseille Cedex 9, France

Received July 23, 1993; Revised Manuscript Received October 25, 1993[●]

ABSTRACT: Cutinases, a group of cutin degrading enzymes with molecular masses of around 22–25 kDa (Kolattukudy, 1984), are also able to efficiently hydrolyse triglycerides (De Geus et al., 1989; Lauwereys et al., 1991), but without exhibiting the interfacial activation phenomenom (Sarda et al., 1958). They belong to a class of proteins with a common structural framework, called the α/β hydrolase fold (Martinez et al., 1992; Ollis et al., 1992). We describe herein the structure of cutinase covalently inhibited by diethyl-*p*-nitrophenyl phosphate (E600) and refined at 1.9-Å resolution. Contrary to what has previously been reported with lipases (Brzozowski et al., 1991; Derewenda et al., 1992; Van Tilbeurgh et al., 1993), no significant structural rearrangement was observed here in cutinase upon the inhibitor binding. Moreover, the structure of the active site machinery, consisting of a catalytic triad (S120, H188, D175) and an oxyanion hole (Q121 and S42), was found to be identical to that of the native enzyme, whereas the oxyanion hole of *Rhizomucor* lipase (Brzozowski et al., 1991; Derewenda et al., 1992), like that of pancreatic lipase (van Tilbeurgh et al., 1993), is formed only upon enzyme–ligand complex formation. The fact that cutinase does not display interfacial activation cannot therefore only be due to the absence of a lid but might also be attributable to the presence of a preformed oxyanion hole.

The natural function of cutinase is to hydrolyze cutin, an insoluble polyester which covers the surface of plants (Kolattukudy, 1984; Ettinger et al., 1987). Cutinase is also able to hydrolyze fatty acid esters and emulsified triacyl glycerol as efficiently as lipases, but without any interfacial activation (Sarda & Desnuelle, 1958; Verger & De Haas, 1976). Functionally speaking, cutinase can therefore be considered as a link between true esterases and true lipases, since it has the capabilities of both families: it is an efficient catalyst both in solution and at the lipidic interface. The X-ray structure of native cutinase has been refined at 1.25-Å resolution (Martinez, 1992; Martinez et al., 1992). Cutinase is a compact one-domain molecule with overall dimensions of about 45 × 30 × 30 Å^3. It has a central β-sheet consisting of five parallel strands covered by five helixes on either side of the sheet. A sixth strand does not belong to the central sheet. To date, the three-dimensional structures of three lipases, from the fungus *Rhizomucor miehei* (RML)[1] (Brady et al., 1990), from human pancreas (HPL) (Winkler et al., 1990; van Tilbeurgh et al., 1992), from *Geotrichum candidum* (GCL) (Schrag et al., 1991), and from *Candida rugosa* (Grochulski et al., 1993) have been elucidated. It has been established that carboxypeptidase-II (Liao & Remington, 1990), acetylcholinesterase (Sussman et al., 1991), and haloalkane dehalogenase (Franken et al., 1991), together with all the lipases belong to a superfamily of proteins with a common structural framework named the α/β hydrolase fold (Ollis et al., 1992). Cutinase also belongs to this class of proteins, of which it is the smallest known member to date (Martinez and Cambillau, unpublished results).

Cutinase is a serine esterase, possessing a catalytic triad. The structural homology existing between cutinase and lipases can be illustrated by the following observations (Martinez et al., 1992): (i) the central β-sheet of cutinase superimposes well with strands 3–7 of the central sheet from RML and HPL; (ii) this β-sheet's superimposition also fits the atoms of the triad involved in the catalytic process (S120, Oγ, H188 Nδ1, D175 Oδ1); (iii) the cutinase catalytic serine 120 has an energe tically unfavourable ϵ conformation ($\phi \cong 60°$, $\psi \cong -120°$), which has also been found to occur in the case of the catalytic serines of other lipases (Derewenda & Derewenda, 1991) and is characteristic of the nucleophilic residues of all the members of the α/β hydrolase class of enzymes (Ollis et al., 1992).

It has been reported that lipases such as RML and HPL undergo considerable conformational changes upon ligand binding: RML structures covalently inhibited by *n*-hexyl phosphonate ethyl ester (Brzozowski et al., 1991) and by E600 (Derewenda et al., 1992) have been solved to 3.0 and 2.6 Å, respectively, and the structure of a ternary HPL–colipase–phospholipid complex has been determined at 3.0 Å (van Tilbeurgh et al., 1993). In the above three structures, the lid covering the active site was displaced by a complex movement, with an amplitude of 12 Å in RML and 27 Å in HPL, leading to an "open" lipase conformation. The *C. rugosa* lipase has an activated open conformation in the absence of any ligand or inhibitor. The conformational change in the lid is thought to be closely related to the interfacial activation phenomenon. In all three enzymes, the rearrangement of the lid results in a large increase in the lipophilic surface, stabilized by interaction with the interface. The exposure to water of these

† This work has been supported by the Bridge T-Lipase project of the EEC (BIOT CT91-0274), by the CNRS IMABIO program, and by the PACA région.

‡ The coordinates have been deposited in the Protein Data Bank.

* Corresponding author.

§ Laboratoire de Cristallisation et Cristallographie des Macromolécules Biologiques.

∥ Laboratoire de Lipolyse Enzymatique.

● Abstract published in *Advance ACS Abstracts,* December 15, 1993.

[1] Abbreviations: HPL, human pancreatic lipase; RML, *Rhizomucor meihei* lipase; PEG, poly(ethylene glycol); E600, diethyl-*p*-nitrophenyl phosphate; cut-E600, diethyl-*p*-nitrophenyl phosphate inhibited cutinase.

0006-2960/94/0433-83$04.50/0

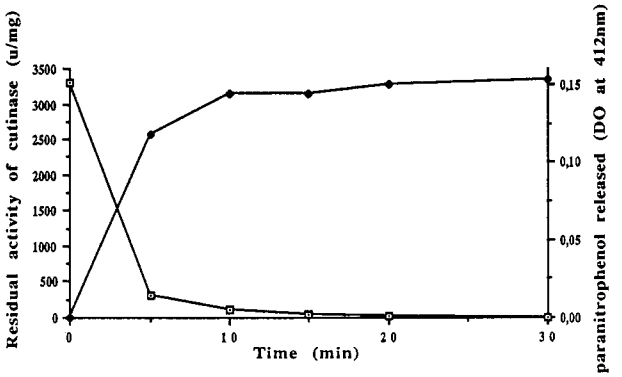

FIGURE 1: Residual activity (□) of cutinase and *p*-nitrophenol release (◆) in the presence of E600 as a function of time.

extensive hydrophobic surfaces would probably be thermodynamically unfavourable in the absence of a lipid–water interface. A second consequence of the movement of the lid in RML and HPL is the formation of the oxyanion hole. As in serine proteases (Kraut et al., 1977), the lipase oxyanion hole provides an electrophilic environment that stabilizes the negative charge generated during the nucleophilic attack on the sissile bond of the substrate. One of the two residues forming the oxyanion holes in both RML and HPL also belongs to the hinge regions of flexible loops the conformation of which changes upon inhibitor binding. Yet, from the evolutionary point of view, the catalytic advantage of a mechanism where the oxyanion hole is not performed and is induced only upon ligand binding is difficult to imagine.

We describe here the structure of cutinase covalently inhibited by diethyl-*p*-nitrophenyl phosphate (E600) and refined at a resolution of 1.9 Å. The aim of this study was to determine whether or not cutinase, which does not display any interfacial activation and does not possess an active site covering lid, has a preformed oxyanion hole. Moreover, this structure provides detailed structural information about the oxyanion hole of a lipolytic enzyme at a higher resolution than that at which lipase–inhibitor complexes have previously been studied.

MATERIALS AND METHODS

Inhibition Experiments and Complex Purification. The recombinant cutinase expression and purification procedures used have been described elsewhere (De Geus et al., 1989; Lauwereys et al., 1991). Lipolytic activity was measured titrimetrically at pH 8.0 and 37 °C with a pH-stat (TTT80 Radiometer) using a tributyrin emulsion as substrate: 0.5 mL of tributyrin was added to 14 mL of a solution containing 0.9% NaCl, 2 mM taurodeoxycholate, and 1.5 μM bovine serum albumin (Gargouri et al., 1989). Cutinase (90 μM) was dissolved in 100 mM Tris, pH 8.0. The inhibitory effects of E600 were monitored by sampling the reaction medium: 0.5-mL aliquots of cutinase were incubated with 0.5 mL of 180 μM (E600) solutions (inhibitor/cutinase molar ratio of 2) (Figure 1). The 1:1 cutinase–E600 complex, which was produced under the same conditions as in the kinetic study, was purified by gel filtration chromatography (FPLC Pharmacia, Superose 12 column).

Crystallization. Crystals of E600 inhibited cutinase were obtained by means of the vapor diffusion technique using PEG 6000 as a precipitant under the same conditions as with the native enzyme: vapor diffusion, 15 mg/mL cutinase–E600, 15–20% PEG6000, 0.1 M MES, pH 6.0 (Abergel et al., 1990; Martinez et al., 1992). The crystals appeared as thin plates

Table 1: Data Collection and Refinement Parameters of the Cutinase–E600 Complex

data collection	
resolution (Å)/distance (mm)	1.9/80
$N°$ observations/$N°$ unique	50967/12970
completeness (%)/R_{sym} (%)[a]	87.6/6.2
redundancy	3.92
% of $I > 3\sigma I$	90
final refinement parameters	
$N°$ of atoms	1446
$N°$ of inhibitor atoms	8
$N°$ of solvent atoms	119
resolution range (Å)	6.0–1.9
$N°$ reflections	12970
R factor ($I/\sigma I > 1$)[b]	18.1%
rms deviations from ideal geometry of the final model	
bond distances (Å)	0.012
bond angles (deg)	2.9
average B factor value (Å^2)	
main-chain atoms	16.9
side-chain atoms	20.0
inhibitor atoms	24.0
solvent atoms	41.5

[a] $R_{sym} = \Sigma_{hkl}\Sigma_{ref}|I_{hkl} - \langle I_{hkl}\rangle|/\Sigma_{hkl}\Sigma_{ref}\langle I_{hkl}\rangle|$. [b] R factor: $\Sigma_{hkl}|F_o - F_c|/\Sigma_{hkl}|F_o|$.

of ca. 0.4 mm × 0.7 mm × 0.1 mm, instead of nicely shaped crystals as with the native enzyme. The space group is also different: the native cutinase crystals are monoclinic, space group $P2_1$, with cell dimensions a = 35.13 Å, b = 67.3 Å, c = 37.05 Å, and β = 94°, whereas the crystals of the E600-inhibited enzyme are orthorhombic, space group $P2_12_12_1$, with cell dimensions a = 40.3 Å, b = 61.1 Å, and c = 72.7 Å. Assuming the asymmetrical unit to contain one molecule, the V_m value is 2.03 Å^3/Da; this is almost identical to the native V_m value of 1.98 Å^3/Da (Matthews, 1968). Due to this dense crystal packing and despite the unfavorable crystal habit, the diffraction extends to 1.9-Å resolution.

Data Collection and Processing. Monochromatic Cu Kα radiation was generated by a Rigaku RU 200 rotating anode at 3.2 kilowatts (40 kV × 80 mA). A total of 90 1° oscillation frames were collected on one crystal at room temperature using the Mar-Research imaging plate scanner at a crystal to detector distance of 80 mm. The data were reduced with the MOSFLM program (Leslie, A, Cambridge, England) and were further processed using the CCP4 suite of programs [CCP4 Program suite, Daresbury Laboratory, Warrington, WA4 4AD, SERC, UK (1986)]. A set of 50 967 reflections was merged to yield 12 970 unique reflections (87.6% complete to 1.9-Å resolution) with an R value calculated from intensities of 6.2% (Table 1).

Structure Determination and Refinement. The orientation of the cutinase–E600 complex in the orthorhombic cell was determined using the molecular replacement option in the program X-PLOR (Brünger et al., 1989). The coordinates of the native cutinase were placed in a P1 cell having the dimensions $a = b = c$ = 60 Å, in a resolution range between 6.0- and 3.0-Å resolution. After PC refinement, solution 807 gave the highest RF_{max} value (0.22) and was used for the X-PLOR translation search. This yielded the correct solution (TF_{max} value 0.19, 15.1σ, R = 0.40). The refinement involved simulated annealing and conjugate gradient minimization with X-PLOR (Brünger et al., 1989). All the display interventions were performed on Silicon Graphics workstations using the TURBO molecular modeling program (Roussel and Cambillau, 1991). The inhibitor E600 is well defined in the electron density map (Figure 2). Water molecules were taken from the native structure and further remodeled on the display

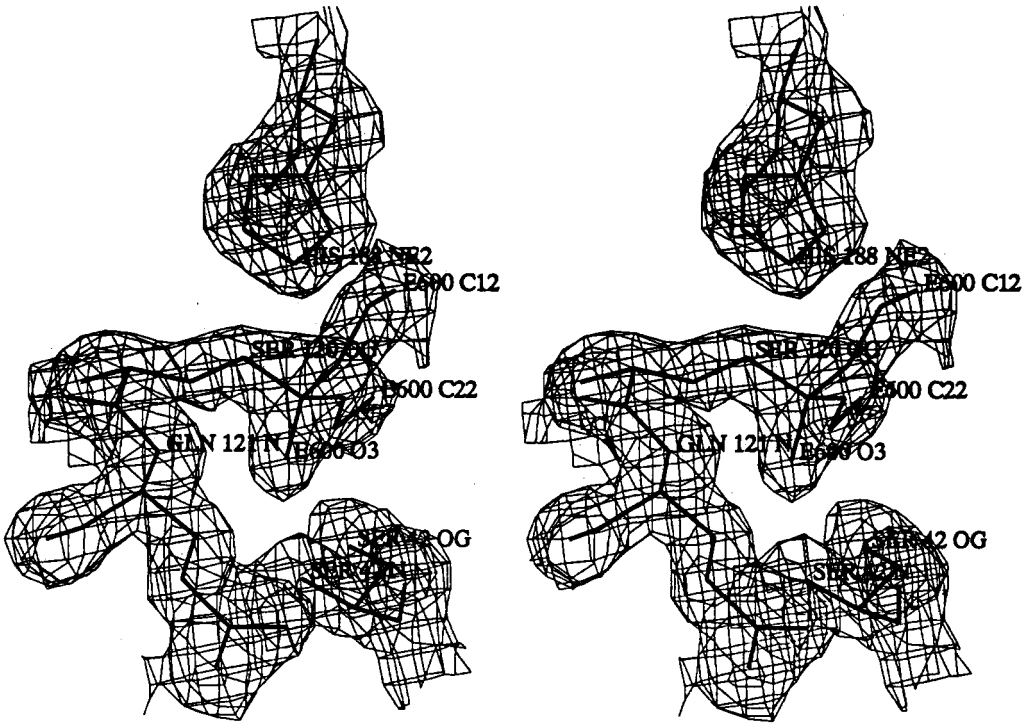

FIGURE 2: Stereoview of the $2F_o - F_c$ electron density map (contoured at 1σ) around the cutinase active site and E600 inhibitor.

Table 2: Root Mean Square Deviations (in Å) between the E600 Inhibited and Native Cutinase, RML, and HPL[a]

	cut–E600	
	Cα atoms	oxyanion hole
native cutinase	0.33 (all)	0.08
native rhizomucor	0.70 (52)	0.30
inhibited rhizomucor	0.73 (55)	0.13
native HPL	0.89 (58)	0.75
inhibited HPL	0.88 (58)	0.11

[a] Deviations have been calculated (i) using the Cα atoms (first column; number of atoms used is in parentheses) or (ii) the catalytic serines and the nitrogen atoms of the oxyanion hole (second column). For cutinases these atoms are Gln 121 N, Ser 42 N, and Ser 120 Oγ.

after each refinement stage. The R factor was 0.181 (6–1.9 Å, $I/\sigma I > 1$) for the final model including 1454 protein and inhibitor atoms and 119 water molecules (Table 1). As with the native cutinase, residues 1–16, which belong to a propeptide, are not visible in the electron density map. In addition, the last two residues could not be identified in the electron density map, being also probably disordered. Luzzati plots imply that the mean positions coordinate eror is between 0.20 and 0.25 Å (Luzzati, 1952).

Structural Superimpositions and Comparisons. The overall structural superimpositions involving cutinase and the open and closed forms of RML and HPL were performed using the RIGID option of TURBO-FRODO. In a first step, a rough rigid body fitting is based on the coordinates of three structurally equivalent atoms. Starting from these new positions, a root mean square fitting is performed between all the Cα atoms lying at a distance of less than a given cutoff value. Gradually decreasing the cutoff value rapidly leads to convergence. The results of this procedure are summarized in Table 2. A second procedure was used to perform an alignment based solely on the active serine Oγ and the nitrogen backbone atoms of the residues involving in the oxyanion hole (Table 2).

RESULTS AND DISCUSSION

Overall Structure and Comparison with the Native Cutinase. The overall structure of cut–E600 is very similar to that of the native crystal structure, as indicated by the very low rms value of 0.33 Å obtained with all Cα atoms (Table 2). The β-sheets are the best conserved parts, whereas minor shifts can be observed in helices and turns (Figure 3). The only significant differences are to be found in a loop (residues 26–31) at the side opposite the active site, with maximum Cα atom deviations of 2.6 Å in the case of residue 27 and of 1.9 Å in that of residue 30 (Figure 3 and 4). This loop is probably flexible, since it displays the highest B factors in the native crystal structure, where it is placed facing the largest crystal solvent channel (Martinez, 1992). In cut–E600 this loop is involved in a crystal packing contact which probably stabilizes a different stable conformation and lowers its B factors. Only minor differences can be observed between the lipid binding sites of the native and inhibited cutinase (see below). The Ramachandran plots (not shown) of native and cut–E600 are nearly identical, demonstrating that no conformational changes occurred upon inhibitor binding. This contrasts with what has been observed for RML (Brzozowski et al., 1991; Derewenda et al., 1992) and HPL (van Tilbeurgh et al., 1993), where conformational changes between the closed and open forms involve displacements of 15 and 33 residues, respectively.

Crystal Packing. Both the native and inhibited cutinase crystals are densely packed. Nevertheless, a great difference in the crystal packing can be observed: in the native structure, the active site loops are tightly involved in crystal contacts, whereas in the inhibited form they are free. One possible reason why a different crystal form was obtained with the cut–E600 complex is that the inhibitor might have introduced steric clashes in the native crystal packing. This is not the case, however: modeling the cut–E600 structure into the native monoclinic packing did not introduce any bad contacts (less than 3.4 Å). The new crystal form of cut–E600 may be due to the existence of a different electrostatic potential in the

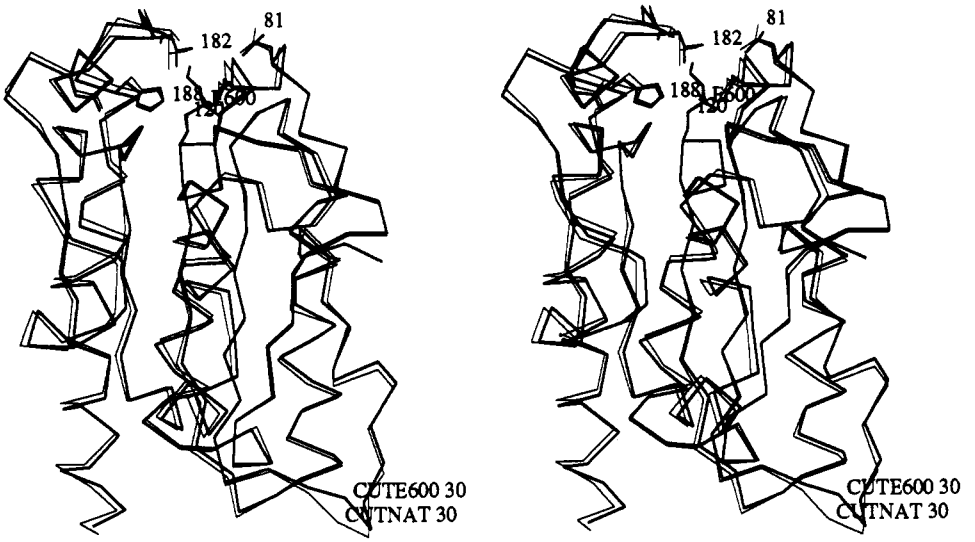

FIGURE 3: Stereoview of E600–cutinase (thick) superimposed on native cutinase (thin). The catalytic triad, the inhibitor, and some residues belonging to the lipophilic interface are displayed.

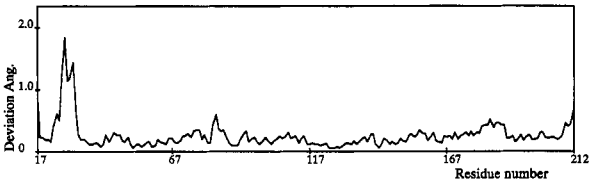

FIGURE 4: Differential plot of the deviation values (in angstroms) between the backbone atoms of E600 inhibited cutinase and native cutinase.

vicinity of the active site, due to the presence of the polarized E600.

The Lipid Binding Site. The lipid binding site of cutinase consists of two loops (residues 80–87 and residues 180–188) above the active site crevice bearing hydrophobic residues L81, G82, A85, L86, P87, L182, I183, and V184 (Figures 3 and 5). Two thin "bridges" formed by side chains of residues Leu 81 and Val 184, and residues Leu 182 and Asn 84 Cβ, partly cover the active site crevice but still leave the catalytic serine accessible to solvent. We have suggested that the absence of the lid masking the active site serine in lipases may explain why cutinase does not display any interfacial activation (Martinez et al., 1992). The E600 inhibitor was accommodated in the active site crevice with only minor changes in the backbone positions of the above described two loops (rms of 0.40 and 0.44 Å, respectively) and in the side chain conformations (Figure 5). The largest observed displacements of the side chains were 0.7 Å with the Leu 182 Cδ2 atom and 1.4 Å with the Leu 81 Cδ2 atom. The active site rim, as measured from the distance between the Cα atoms of Leu 81 and Val 184, is only 0.8 Å wider in the E600 bound form than in the native structure. Moreover, this small difference may be due to differences in the crystal packing.

The Catalytic Triad and the Inhibitor. The active site of cutinase contains the catalytic triad residues Ser 120, His 188, and Asp 175. A water molecule is hydrogen bound with three main chain atoms of cutinase (Leu 176 NH, Ala 185 NH, and Ile 183 O), and its fourth valency is hydrogen bound to the Asp 175 Oδ1 atom, which favors the proper orientation of this residue. Ser 120, which is located in a β-hairpin, has the ε conformation ($\phi = 60°$ and $\psi = -123°$), often found at the second position in these types of β-hairpins (Derewenda & Derewenda, 1991). After the central β-sheets of RML, HPL, and native and complexed cutinase were superimposed,

Table 3: E600 Inhibited Cutinase: Contacts between the E-600 Inhibitor and Cutinase (<4.0 Å)

E-600 inhibitor

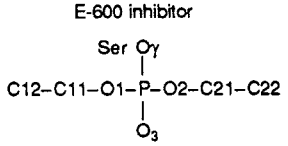

E600 atoms	cutinase atoms	distance (Å)
O1	Asn 84 Oδ1	3.60
O1	Asn 84 Nδ2	3.62
C11	Val 184 Cγ2	3.85
C12	Leu 182 Cδ2	3.55
O2	His 188 Nε2	3.21
C21	Tyr 119 Cε2	3.94
C21	His 188 Nε2	3.74
C22	Tyr 119 Cz	3.83
C22	Tyr 119 OH	3.29
C22	His 188 Nε2	3.60
O3	Ser 42 N	2.86
O3	Ser 42 Oγ	2.68
O3	Gln 121 N	2.87

the catalytic triads of these three enzymes were found to almost overlap, especially the atoms involved in the catalytic process (Oγ, Nε, Oδ). The topological origin of the catalytic residue Asp 176 of HPL differs from that of the corresponding aspartates from RML (Asp 203) and cutinase (Asp 175) (Martinez et al., 1992; Ollis et al., 1992; Schrag et al., 1992).

The structure of the catalytic triad is basically the same in the native and inhibited enzyme (Figure 6). The largest movement is observed at the His 188 Nε2 atom (0.36 Å), which interacts with the E600 C11 atom (Table 3). A water molecule, located in front of Ser 120 in the native structure, has been replaced by the inhibitor. The inhibitor O3 atom is hydrogen bound with residues 121 and 42, forming the oxyanion hole (see below). It establishes van der Waals contacts with residue His 188 from the catalytic triad, with residue Tyr 119, and with residues Val 177, Leu 182, and Val 184 of the lipid binding site (Table 3).

The Oxyanion Hole. Phosphorylating agents have a longstanding tradition in studies on serine protease mechanisms. The covalent adduct with the active serine is believed to mimic the tetrahedral intermediate of the reaction (Kraut, 1977). Crystallographic analysis of these complexes has made it possible to identify the main chain nitrogens that form the

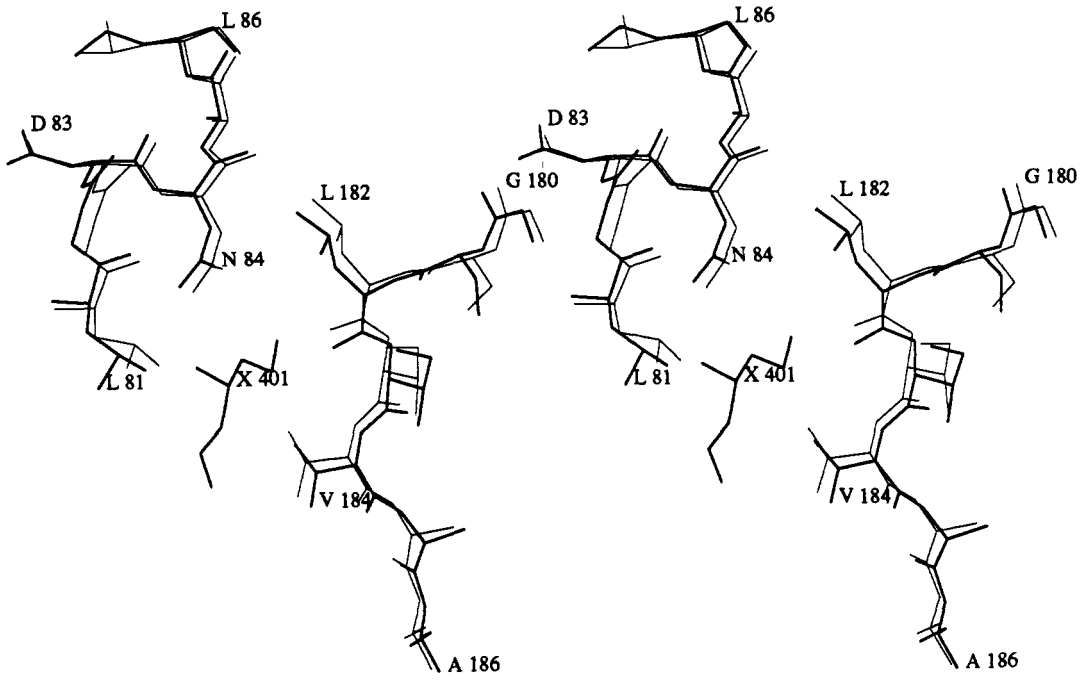

FIGURE 5: Stereoview of the lipid binding site of E600–cutinase (thick) superimposed on that of native cutinase (thin). The E600 inhibitor is also shown (401).

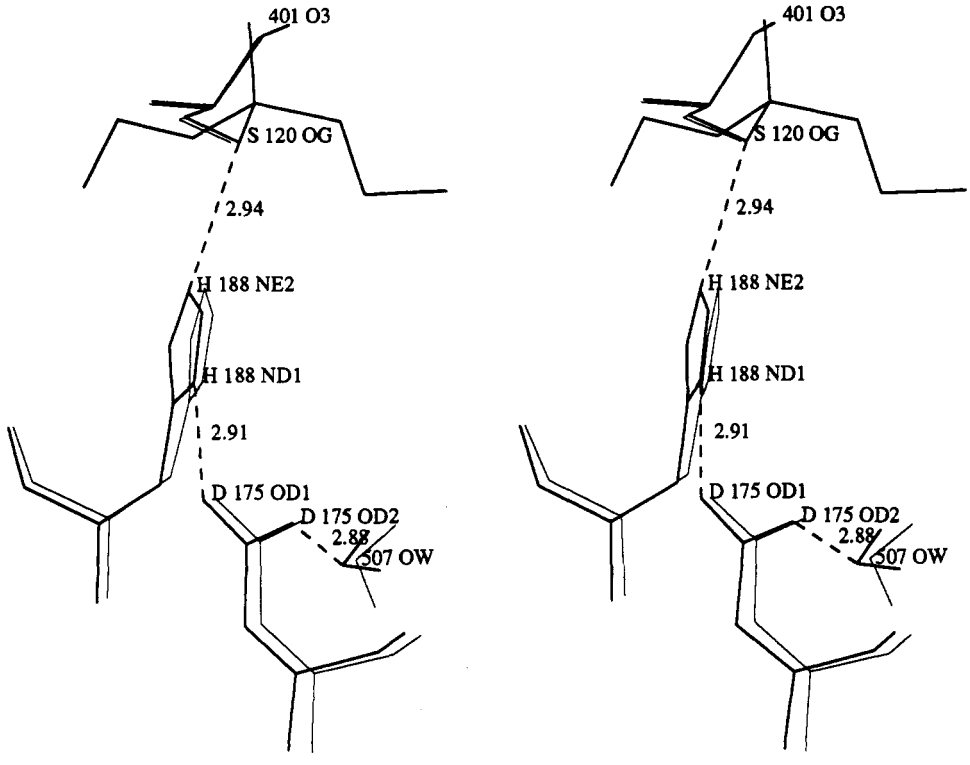

FIGURE 6: Stereoview of the catalytic triad of the E600–cutinase (thick) superimposed on that of native cutinase (thin). The E600 inhibitor is also shown (401) as well as the triad bound water molecule (507).

oxyanion hole. These nitrogen atoms lie within hydrogen-bonding distance from the phosphate or phosphonate oxygen. Analysis of the environment of the phosphate oxygen in the cut–E600 structure confirms the presence of an oxyanion hole in cutinase and establishes its nature. The main chain nitrogens of Ser 42 and of Gln 121, the residue next to the catalytic serine, are within hydrogen-bonding distance of the E600 O3 atom (Table 4). The Ser 42 Oγ atom is at a distance of 2.68 Å, but the geometry is not optimal for hydrogen bonding. The position of the Ser 42 side chain is further stabilized by hydrogen bonds with Asn 84 NH2 and with Gln 121 NH2 (Figure 7a).

Two inhibited RML structures (Brzozowski et al., 1991; Derewenda et al., 1992) made it possible to locate the backbone nitrogen atom of Leu 145 next to the active site serine and that of Ser 82 as part of the oxyanion hole. The Ser 82 Oγ, which is the equivalent of Ser 42 Oγ in cutinase, may also be hydrogen bonded to the phosphate oxygen and may therefore contribute to the anion stabilization. The Ser 82 Oγ atom is stabilized by only one interaction with Asp81 (superimposing

Table 4: Distances (Å) between Atoms of the Oxyanion Hole[a]

	PO–N1	PO–N2	PO–Oγ	Oγ–X1	Oγ–Nε2 Q121
native cutinase	2.89 Q121	2.83 S42	2.65 S42	3.23 NH2 N84	3.02
cutinase E600	2.87 Q121	2.86 S42	2.68 S42	2.96 NH2 N84	3.02
native RML	2.60 L145	3.78 S82	2.47 S82	11.4 OD1/2 D91	
inhibited RML	3.03 L145	3.01 S82	3.02 S82	2.39/3.04 OD1/2 D91	
native HPL	3.21 L153	2.50 F77			
inhibited HPL	2.78 L153	2.95 F77			

[a] O refers to the oxygen atom of the phosphate E600 or the phosphonate (RML only); N1 refers to the nitrogen atom of the oxyanion hole residue next the catalytic serine. N2 refers to the nitrogen atom of the oxyanion hole residue in the hinge region; Oγ refers to the side chain Oγ atom of the residue next the catalytic serine; X1 is the second ligand of Oγ. The distances between inhibitor oxygen atom in the native cutinase, RML, and HPL and in the inhibited form of HPL are calculated using the E600 inhibitor coordinates aligned onto these structures.

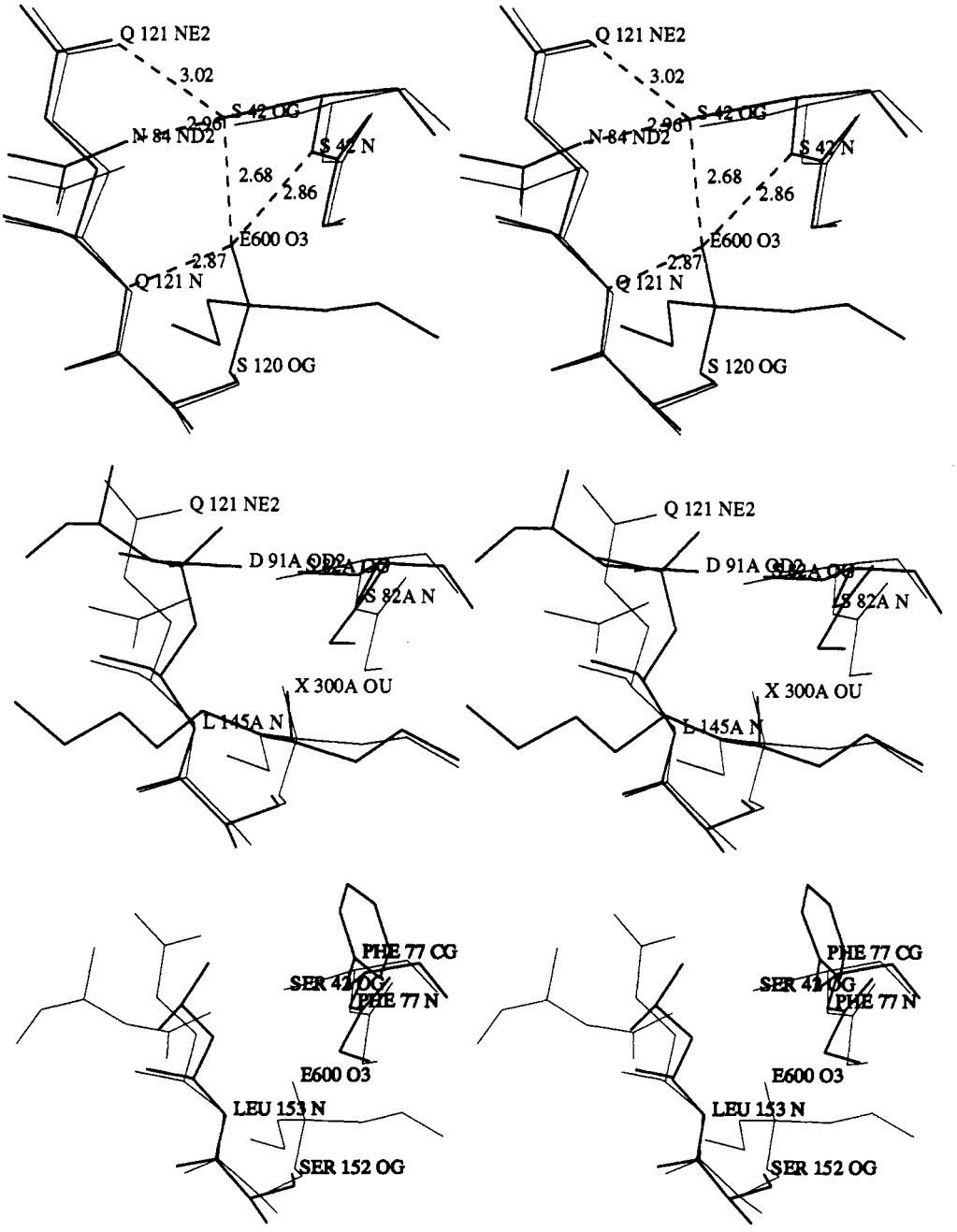

FIGURE 7: (a, top) Stereoview of the oxyanion hole of E600–cutinase (thick) superimposed on that of native cutinase (thin). The E600 inhibitor is also shown as well as the hydrogen bonds involved in the oxyanion hole formation. (b and c) Stereoview of the oxyanion hole of the inhibited RML (b, middle) (thick) and that of the inhibited HPL (c, bottom) (thick) superimposed on that of the E600 inhibited cutinase (thin). Those residues involved in the oxyanion hole formation have been labeled.

onto Asn 84 in cutinase), in contrast with the two above-mentioned hydrogen bonds of the corresponding Ser42 Oγ in cutinase. Winkler et al. (1991) hypothesized that the oxyanion hole in HPL may be formed by the main chain nitrogens of Phe 77 and Leu 153 (the residue adjacent to the active site serine). This was confirmed in a study where the structure

of a ternary lipase–colipase–phospholipid complex was determined (van Tilbeurgh et al., 1993). Nevertheless HPL, unlike RML and cutinase, has a phenylalanine at that position (Phe 77) and therefore cannot provide a third partner for oxyanion stabilization.

The atoms involved in cutinase oxyanion hole formation do not move upon inhibitor binding (rms value of 0.08 Å compared to the native structure), whereas significant displacements occur in RML and HPL upon inhibition. It has been established that the backbone nitrogen atoms of Ser 82 in RML and of Phe 77 in HPL are brought into the catalytically competent position by considerable conformational changes in active site loops: Ser 82 in RML belongs to the hinge region of the lid, while in HPL Phe 77 is not part of the lid but belongs to another mobile surface loop (Derewenda et al., 1992; van Tilbeurgh et al., 1993). After inhibition, the active serine Oγ and the oxyanion main chain nitrogens of RML and HPL superimpose perfectly on those of cutinase (Table 2; Figure 7b,c). These findings mean that the oxyanion hole is preformed in cutinase instead of being induced by ligand binding.

Conclusion. The interfacial activation of triglyceride lipases has been attributed to the conformational change in a lid covering the catalytic residues. Formation of the oxyanion hole upon substrate binding may complete the structural picture. The reason for the opening of the lid is easy to understand: it leads to a huge increase in the lipophilic surface of the lipase and gives access to the catalytic triad. A ready-made open lipase would probably be much less soluble. The reason why the oxyanion hole of true lipases is not preformed is an intriguing question. The lipases oxyanion hole residues may not be involved in interface induced rearrangements, as in the case for the catalytic triad.

ACKNOWLEDGMENT

We thank Prof. Guy Dodson for providing us with the RML inhibited structure and Dr. M. Lauwereys for the gift of recombinant cutinase.

REFERENCES

Abergel, C., Martinez, C., Fontecilla-Camps, J., Cambillau, C., De Geus, P., & Lauwereys, M. (1990) *J. Mol. Biol. 215*, 215–216.

Brady, L., Brzozowski, A., Derewenda, Z. S., Dodson, R., Dodson, G., Tolley, S., Turkenburg, J. P., Christiansen, L., Huge-Jensen, B., Norskov, L., Thim, L., & Menge, U. (1990) *Nature 343*, 767–770.

Brzozowski, A. M., Derewenda, U., Derewenda, Z. S., Dodson, G., Lawson, D., & Turkenburg, J. P. (1991) *Nature 351*, 491–494.

Brünger, A. T., Karplus, M., & Petsko, G. (1989) *Acta Crystallogr. A45*, 50–61.

De Geus, P., Lauwereys, M., & Matthyssens, G. (1989) European Patent Application No. PCT 89.400.462.1.

Derewenda, U., Brzozowski, A. M., Lawson, D., & Derewenda, Z. S. (1992) *Biochemistry 31*, 1532–1541.

Derewenda, Z. S., & Derewenda, U. (1991) *Biochem. Cell Biol. 69*, 842–851.

Ettinger, W. F., Thukral, S. K., & Kolattukudy, P. E. (1987) *Biochemistry 26*, 7883–7892.

Franken, S. M., Robezoom, H. J., Kalk, K. H., & Dijkstra, B. W. (1991) *EMBO J. 10*, 1297–1302.

Gargouri, Y., Moreau, H., & Verger, R. (1989) *Biochim. Biophys. Acta 1006*, 255–271.

Grochulski, P., Li, Y., Schrag, J. D., Bouthillier, F., Smith, P., Harrison, D., Rubin, B., & Cygler, M. (1993) *J. Biol. Chem. 268*, 12843–12847.

Kolattukudy, P. E. (1984) in *Lipases* (Borgström, B., & Brockman, H., Eds.) pp 471–504, Elsevier, Amsterdam.

Kraut, J. (1977) *Annu. Rev. Biochem. 46*, 331–358.

Lauwereys, M., de Gues, P., de Meutter, J., Stanssens, P., & Matthyssens, G. (1991) in *Lipases—Structure, Mechanism and Genetic Engineering* (Alberghina, L., et al., Eds.) Vol. 16, pp 243–251, VCH, Weinheim.

Liao, D.-L., & Remington, S. J. (1990) *J. Biol. Chem. 265*, 6528–6531.

Luzzati, V. (1952) *Acta Crystallogr. 5*, 802–810.

Martinez, C. (1992) Thèse de doctorat, Université de Paris XI, Orsay.

Martinez, C., de Geus, P., Lauwereys, M., Matthyssens, G., & Cambillau, C. (1992a) *Nature 356*, 615–618.

Martinez, C., Stanssens, P., de Geus, P., Lauwereys, M., & Cambillau, C. (1992b) *Protein Eng. 6*, 157–165.

Matthews, B. W. (1968) *J. Mol. Biol. 33*, 491–497.

Ollis, D. V., Cheah, E., Cygler, M., Dijkstra, B., Frolow, F., Franken, S. M., Harel, M., Remington, S. J., Silman, I., Schrag, J., Sussman, J. L., Verschueren, K. H. G., & Goldman, A. (1992) *Protein Eng. 5*, 197–211.

Pathak, D., & Ollis, D. (1990) *J. Mol. Biol. 214*, 497–525.

Roussel, A., & Cambillau, C., (1991) in *Silicon Graphics Directory*, p 97, Mountain View, CA.

Sarda, L., & Desnuelle, P. (1958) *Biochim. Biophys. Acta 30*, 513–521.

Schrag, J. D., Li, Y., Wu, S., & Cygler, M. (1991) *Nature 351*, 761–764.

Schrag, J. D., Winkler, F. K., & Cygler, M. (1992) *J. Biol. Chem. 267*, 4300–4303.

Sussman, J. L., et al. (1991) *Science 253*, 872–879.

van Tilbeurgh, H., Sarda, L., Verger, R., & Cambillau, C. (1992) *Nature 359*, 159–162.

van Tilbeurgh, H., Egloff, M.-P., Martinez, C., Rugani, N., Verger, R., & Cambillau, C. (1993) *Nature 362*, 814–820.

Verger, R., & de Haas, G. H. (1976) *Annu. Rev. Biophys. Bioeng. 5*, 77–117.

Winkler, F. K., D'Arcy, A., & Hunziker, W. (1990) *Nature 343*, 771–774.